

Experimental Study of SBPWM for Z-Source Inverter Five Phase

M.S.Bakar*, N.A.Rahim**, H.Daniyal*, K.H.Ghazali***

* SuPER, Faculty of Electrical & Electronics Engineering, University Malaysia Pahang

** UMPEDAC, Faculty of Engineering, University Malaya

*** ViSIS, Faculty of Electrical & Electronics Engineering, University Malaysia Pahang

Article Info

Article history:

Received Oct 6, 2014

Revised Dec 3, 2014

Accepted Dec 25, 2014

Keyword:

Five-phase inverter

Modulation index

Pulse width modulation

Total harmonic distortion

Z-source inverter

ABSTRACT

On the basis of a conventional Z-source inverter, this paper presents an extension of the existing study about a driving scheme implementation of a simple boost pulse width modulation under open loop system for five phase two level system. The impact of design parameter (fixed modulation index and switching frequency) versus performance parameter (capacitor voltage, inductor current, total harmonic distortion and DC link voltage) are studied and analysed. To validate the advantages of Z-source five-phase inverter, the driving scheme are simulated using Matlab/Simulink and verified with real-time target board eZdspTMTMS320F28335. From the study, it was found that under specified modulation index and switching frequency, the THD of an output current fulfilled the EN61000-3-2 standard.

Copyright © 2015 Institute of Advanced Engineering and Science.
All rights reserved.

Corresponding Author:

M.S.Bakar,

SuPER, Faculty of Electrical & Electronics Engineering, Pekan Campus,

University Malaysia Pahang, 26600, Pekan, Pahang, Malaysia.

Email: shafie@ump.edu.my

1. INTRODUCTION

Over the past forty years, there has been a dramatic increase in the use of fivephase voltage source inverter (VSI) fed motor drive [1], a well-known system that can be fabricated using low-cost, high-performance insulated gate bipolar transistor (IGBT) modules or intelligent power modules [2]. Recent developments in VSI fed motor drive have heightened the need for analyzing the topology, driving scheme, control technique and application. One type of VSI fed motor drive is the Z-source inverter (ZSI), as proposed by F.Z. Peng [3]. Other researcher found [4] that ZSI has progressed actively with the electric vehicle whereby the drive voltage is stress in huge and its investigation has also become a continuing concern within the scope of multiphase systems. There is a large volume of published studies describing the roles of ZSI in multiphase systems [5]–[7]; however, this paper focuses only on the fivephase inverter since it commonly used and the smallest number of phases in a multiphase systems [8].

ZSI has the capability to resolve mutual problems either in VSI fed or in current source inverter (CSI) fed motor drive, which are [3]:

- Issues in bucking and boosting mode operation. The output produced by a H-bridge inverter is restricted either to greater than or smaller than the input voltage. By controlling the modulation index (M_i) of the driving scheme, there is a range of M_i that can be used for bucking and boosting purposes.
- The input circuit to the H-bridge inverter is fixed. During bucking mode, a specific buck converter circuit must be added, while during boosting mode, a boost converter circuit must be provided. With ZSI, bucking and boosting modes can be provided using with similar topology and single stage conversion.

- c) The effect of electromagnetic interference (EMI) in conventional inverter system contributes to the level of harmonic content. By avoiding a dead time application in ZSI for each of the upper and lower leg would minimise the harmonic content in the system.

Given ZSI's many benefits, this paper presents an investigation as follows. Section 2 describes the motivation and research goal using ZSI fivephase that employs a simple boost pulse width modulation (SBPWM). Detailed explanation of the SBPWM process is presented in Section 3. Simulation and experimental results are illustrated in Section 4 to show that the harmonic content based on the EN61000-3-2 standard for class D order is complied. In Sections 5, 6 and 7, the details experimental test platform is clarified under open loop system with selected component conditions. Conclusions are given in Section 8.

2. MOTIVATION & RESEARCH GOAL

Pulse width modulation (PWM) has become a vital and significant element of a multiphase system [9]. A preliminary work conducted using PWM for four-phase ZSI was undertaken by [2]. In the study, PWM for single, three and four phases under continuous and discontinuous mode were analysed using simulation platform. The hardware verification was done under three-phase system.

In 2013, A. Kouzou [5] reported the use of PWM in multiphase systems, in which case a maximum boost control (MBC) strategy for multiphase system from 3, 5, 7, 11, 13, 15, 17, 19 and 21 phases under simulation task were employed. In the experimental setup, the researchers fed two parallel loads, a five-phase resistive load and a five-phase induction machine to verify the simulation result. They found that the system could accomplish any desired output multiphase AC voltage whose magnitude is greater than the input DC voltage [5]. The performance parameters of the system was also improved, which include the decrease in the Z-source capacitor voltage and Z-source inductor current ripple [5].

The findings above became the motivations for this research to investigate other PWM driving schemes, such as SBPWM with DSP based for ZSI fivephase. SBPWM is a well-known driving scheme in ZSI, as it mathematically uncomplicated [10], easy to implement [10], and has been tested using many new topologies of ZSI [11]–[15].

3. BACKGROUND ZSI FIVE-PHASE TOPOLOGY AND ITS OPERATION

The topology of ZSI fivephase used in this research is shown in Figure 1. The load is connected in a star formation and the load on each phase consists of a parallel connection of a resistance, a capacitance and an inductance. The front end of the topology consists of a DC input voltage that is assumed to be a ripple-free constant DC voltage source, an ultrafast diode used to prevent circulation of the reverse current towards the DC power supply, a Z-source network acting as a second order filter (consisting of two identical capacitors and inductors) and an H-bridge inverter (consisting of ten IGBTs).

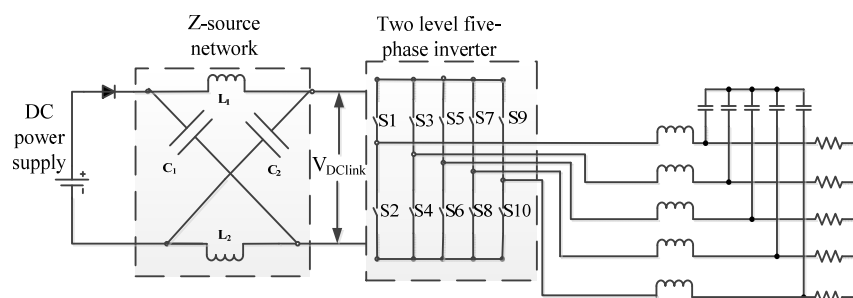


Figure 1. Z-source five phase inverter application under star formation

A derivation of ZSI five phase is similar to that of a conventional five phase VSI but, referring to Figure 1, with the addition of a Z-source network as an input to the five phase H-bridge inverter makes the analysis different from that of the conventional five phase VSI. The Z-source network voltage of the ZSI five phase must satisfy the following equalities [3]:

$$V_{L_1} = V_{L_2} = V_L \quad (1)$$

$$V_{C_1} = V_{C_2} = V_C \quad (2)$$

Two levels of ZSI five phase produces three states [16], namely, normal state (active state), non-shoot through state (zero state) and shoot through state, which represent synchronized switching condition for any two power devices within the leg. In active and non-shoot through state the ZSI five phase operates under conventional PWM strategy. However, in the shoot-through state, the output five phase H-bridge inverter terminals are shorted at both the upper and the lower switching devices of any of the phase legs [16], while simultaneously, the capacitor voltage is boosted by receiving the energy from the inductor [17]. The total number of shoot-through states of ZSI five phase dealing with the standard formulation is $2^n - 1$ [5], where n represents the number of phases. Thus, for ZSI five phase, the available total shoot-through states are 31, as shown in Table 1 that has been adopted from [2]. The shoot-through states short-circuit all five AC output terminals and produce 0 V across the AC load. The odd and even number of switches represent the upper and lower switches, respectively.

Table 1. Switching state shoot-through for Z-source phase inverter (!SX represents complement of SX, where X=1, 3, 5, 7 or 9).

State	S1	S2	S3	S4	S5	S6	S7	S8	S9	S10
F1(0V)	1	1	S3	!S3	S5	!S5	S7	!S7	S9	!S9
F2(0V)	S1	!S1	1	1	S5	!S5	S7	!S7	S9	!S9
F3(0V)	S1	!S1	S3	!S3	1	1	S7	!S7	S9	!S9
F4(0V)	S1	!S1	S3	!S3	S5	!S5	1	1	S9	!S9
F5(0V)	S1	!S1	S3	!S3	S5	!S5	S7	!S7	1	1
F6(0V)	1	1	1	1	S5	!S5	S7	!S7	S9	!S9
F7(0V)	1	1	S3	!S3	S5	!S5	S7	!S7	1	1
F8(0V)	1	1	S3	!S3	S5	!S5	1	1	S9	!S9
F9(0V)	1	1	S3	!S3	S5	!S5	S7	!S7	1	1
F10(0V)	1	1	S3	!S3	1	1	S7	!S7	S9	!S9
F11(0V)	S1	!S1	1	1	1	1	S7	!S7	S9	!S9
F12(0V)	S1	!S1	1	1	S5	!S5	1	1	S9	!S9
F13(0V)	S1	!S1	1	1	S5	!S5	S7	!S7	1	1
F14(0V)	S1	!S1	S3	!S3	1	1	1	1	S9	!S9
F15(0V)	S1	!S1	S3	!S3	1	1	S7	!S7	1	1
F16(0V)	S1	!S1	S3	!S3	S5	!S5	1	1	1	1
F17(0V)	1	1	1	1	S5	!S5	1	1	S9	!S9
F18(0V)	1	1	1	1	S5	!S5	S7	!S7	1	1
F19(0V)	1	1	S3	!S3	1	1	1	1	S9	!S9
F20(0V)	1	1	S3	!S3	1	1	S7	!S7	1	1
F21(0V)	1	1	S3	!S3	S5	!S5	1	1	1	1
F22(0V)	S1	!S1	1	1	1	1	1	1	S9	!S9
F23(0V)	S1	!S1	1	1	1	1	S7	!S7	1	1
F24(0V)	S1	!S1	1	1	S5	!S5	1	1	1	1
F25(0V)	S1	!S1	S3	!S3	1	1	1	1	1	1
F26(0V)	1	1	1	1	1	1	1	1	S9	!S9
F27(0V)	1	1	1	1	1	1	S7	!S7	1	1
F28(0V)	1	1	1	1	S5	!S5	1	1	1	1
F29(0V)	1	1	S3	!S3	1	1	1	1	1	1
F30(0V)	S1	!S1	1	1	1	1	1	1	1	1
F31(0V)	1	1	1	1	1	1	1	1	1	1

4. SIMPLE BOOST PWM WORKING PRINCIPLE

The SBPWM was the early driving scheme in ZSI. The scheme was approved for boosting criteria by turning the zero state into shoot-through state, keeping the active state unchanged, maintaining the output load in sinusoidal form and, most important, boosting the DC link voltage from the shoot-through affect. This driving scheme was used to control the shoot-through duty ratio, in which the maximum shoot-through duty ratio is limited by $(1-M_i)$ [3], [18]. As noted by [3], [18], the relationship between M_i and boost factor (B) under SBPWM that is used to determine voltage gain (G) can be described as:

$$\frac{V_{AC}}{V_{DC}/2} = M_i B \quad (3)$$

Where V_{AC} is the output peak phase voltage and V_{DC} is the input DC voltage. By rearranging Equation (3), the DC link voltage can be obtained under specific M_i as:

$$V_{DClink} = BV_{DC} \quad (4)$$

Where V_{DClink} is the voltage across the input to the H-bridge inverter. The effect of M_i and V_{DClink} will be analyzed and compared with the result of simulation established on the Matlab/Simulink and the result of experimental. In SBPWM, a shoot-through periods are generated by a few processes [19]. A sample for the driving scheme of SBPWM for phase A is derived as shown in Figure 2. First, the two constant signals (upper and lower level) are compared to the peak of a triangular carrier signal. Second, the carrier signal is compared to a 50Hz sinusoidal reference signal as in conventional PWM. Third, the product of the two comparisons is loaded into the logical process to obtain a final PWM for ZSI five phase. The PWM signals are then sent to control the power devices (IGBTs) through isolation and gate drive.

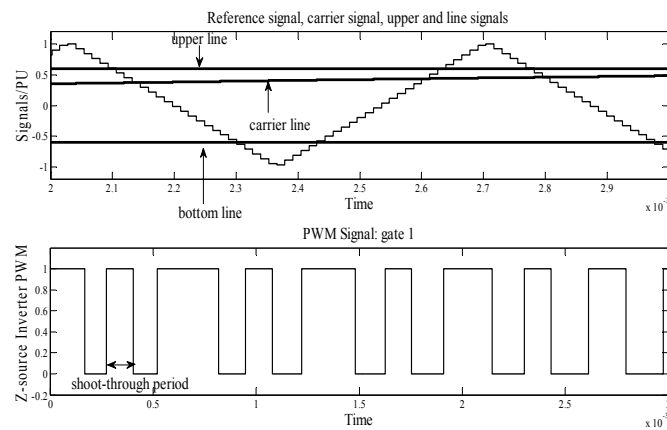


Figure 2. Driving scheme ZSI fivephase for Phase A

5. DESIGN CONSIDERATIONS FOR KEY COMPONENTS

To verify the feasibility of the topology, a maximum 2-kW (under star formation) laboratory prototype operated at 1.5kHz switching frequency was built. The simulation and experimental results will be shown and discussed in the next section. The design considerations for the key components for this research will be discussed in detail as follows. The laboratory prototype for ZSI fivephase used in this study, shown in Figure 3 and Figure 4, is capable of performing open-loop operation for five-phase resistive load with variable M_i up to a maximum of 125 Watt/phase (maximum of 625 Watt under star formation). Table 2 shows the detail parameters of the laboratory prototype.

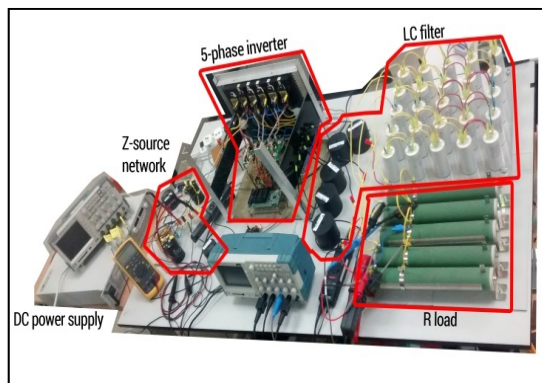


Figure 3. The laboratory prototype of ZSI five-phase for linear load and LC filter

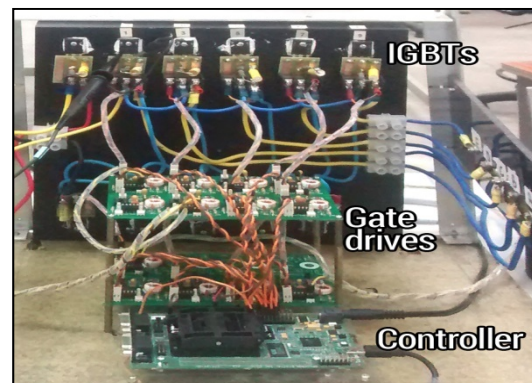


Figure 4. Closer view of the IGBTs, gate drives and controller systems

Table 2. Z-source inverter five phase system parameters for the simulation and experiment

Parameter	Value
DC input voltage (V_{DC})	40 V
Sampling time	13 μ sec
Switching frequency (f_s)	1.5 kHz
Fundamental frequency	50 Hz
Z-source capacitor (C_1 & C_2)(V_{DC})	1000 μ F, 400 V
Z-source inductor (L_1 & L_2) (A_{rms})	1000 μ H, 10.6 A
Load capacitance/phase (V_{AC})	30 μ F, 420 V
Load inductance/phase (A_{rms})	5 mH, 10 A
Load resistance/phase	25 Ω , 125 Watt

5.1. Component Selection in Z-source Network

The selection of Z-source network component (capacitor and inductor) in ZSI five phase is not straight forward. The fundamental concept that needs to be considered is that the capacitor voltage is assumed to be constant [20]. This is done by selecting a large enough capacitor so that its ripple voltage is sensible low [20]. Once the capacitor has been decided, the inductor is selected using a trial-and-error procedure as its value is related to that of the capacitor. According to the procedure, after fulfilling all the requirements, the value of the inductor can be incrementally increased while following the procedure so as to meet the requirement.

5.2. Main controller ezDSP TMS320F28335

A eZdsp™ TMS320F2812 DSP was selected to apply the control algorithm as it has a 32-bit CPU performing at 150MHz [21], [22]. A feature of this target board is its general purpose input-output (GPIO) ports: GPIOA, B and C that contains 88 pins. These ports are able to integrate with the target support package tool box in Matlab/Simulink and easily loaded to the target board. In this study, the development of SBPWM was performed in the Matlab/Simulink platform and been connected to the specific port of GPIO by setting the appropriate pin assignment. The logical algorithm has also been developed in the Matlab/Simulink platform to gain a final signal of PWM.

6. PERFORMANCE INDICATOR

In this research, the focus is on the system's performance indicator, which has been defined as its performance and design parameters. Performance parameter [23] is associated with the output control (THD of output voltage/current, and V_{DClink} , voltage capacitor and inductor current of Z-source network), while design parameter is related to the input control (M_i and switching frequency).

6.1. Performance Parameter

Total harmonic distortion (THD) is generally used to measure distortion for an inverter [24]. In this study, the output current THD of the system was made to comply with EN61000-3-2 standard, which stated that the maximum permissible current of the 3rd harmonic is 2.3 A [25].

6.2. Design Parameter

The M_i used in this research is in the range of 0.56 to 1.0 (linear modulation). The results obtained from simulation show that the modulation indices were capable of boosting and producing voltage gains that are equal to that predicted from theory as many parameters are set as ideal components in the simulation platform. However, the voltage gains obtained from the experiments are only equal to that predicted from theory when M_i in the range of 0.6 to 1.0 is used. Smaller M_i results in bigger shoot-through period that causes more current to flow through the IGBT. Other factors such as the soldering technique used in the IGBT pre-module, interference from the length of the wiring system among the passive components and equipment noise also affect the shoot-through period, which contribute to the overall interference of the system. To stabilize the system, the problem is compensated by limiting the shoot-through period, which can be achieved by confining the range of M_i is used.

The relationship between M_i , shoot-through duty ratio (D_0) and voltage gain (G) can be expressed as follows [10]:

$$D_0 = 1 - M_i \quad (5)$$

$$G = \frac{M_i}{1 - 2D_0} \quad (6)$$

Equation (5) shows that D_0 is inversely proportional to M_i . Rearranging Equation (6) results in the following expression [10]:

$$M_i = \frac{G}{2G - 1} \quad (7)$$

And V_{DClink} can be determined as:

$$V_{DClink} = (2G - 1)V_{DC} \quad (8)$$

Based on Equation (7) and (8), the smaller the value of M_i , the bigger the value of V_{DClink} achieved, and the bigger the current flows through the IGBT.

7. RESULTS AND DISCUSSIONS

7.1. Simulation Results

To verify the effectiveness of the topology, simulations were performed to validate the consistency of the boost factor, voltage gain, the limitation of the capacitors voltage stress and the inductors current ripple using Matlab/Simulink. The simulation model uses the parameter as stated in Table 2, with two levels fivephase H-bridge inverter that consists of ten (10) IGBTs. The switching frequency and the sampling frequency are $f_s = 1.5$ kHz and $f_{sam} = 76$ kHz, respectively. The M_i is 0.62, which results in $D_0 = 0.38$, $B = 4.17$ and $G = 2.58$. The theoretical peak output phase voltage to neutral is $V_{AC} \approx 51.7$ V, while that obtained from the simulation, shown in Figure 5, is $V_{AC(simulation)} \approx 55.6$ V with THD = 2.0%. Figure 6 shows the output current of the resistive load that is connected in star formation. Under steady state condition, THD = 2% and the peak magnitude = 1.96A. Under steady state condition, the theoretical DC link voltage $V_{DClink} \approx 166.8$ V, while that obtained from the simulation $V_{DClink(simulation)} \approx 150$ V, as shown in Figure 7. This difference is believed due to the parasitic effects that cause in reducing the voltage gain the experiment.

The steady state condition for the capacitor voltage is 93.6 V, while the average value of inductor current under steady state is 7.14 A, as shown in Figure 8. The ripple capacitor voltage obtained in this simulation is 0.92%, while the ripple inductor current gained for this result is 10A, which is considered as high. The results above should be considered as a great advantage for using ZSI five phase instead of the conventional five-phase inverter since the simulation result nearly equaled that of the theoretical values.

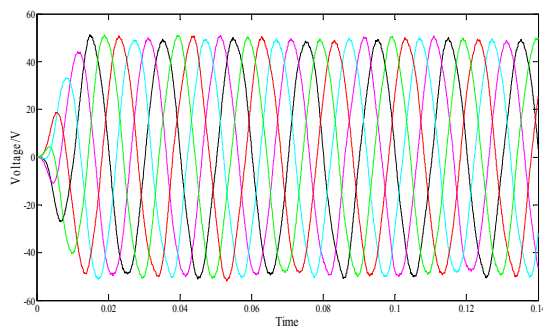


Figure 5. Five-phase output voltage at $M_i = 0.62$, $V_{DC} = 40$ V at $f_s = 1.5$ kHz and sampling time = 13 μ sec with 25 resistiveohm load

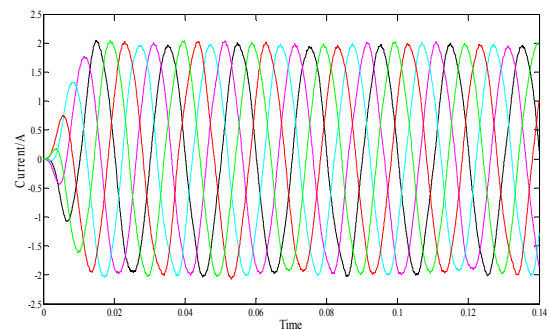


Figure 6. Five-phase output current at $M_i = 0.62$, $V_{DC} = 40$ V at $f_s = 1.5$ kHz and sampling time = 13 μ sec with 25 resistiveohm load

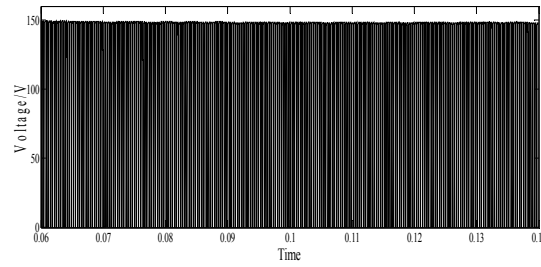


Figure 7. Test result V_{dclink} at $M_i = 0.62$, $V_{DC} = 40$ V at $f_s = 1.5$ kHz and sampling time = 13 μ sec with 25 resistiveohm load

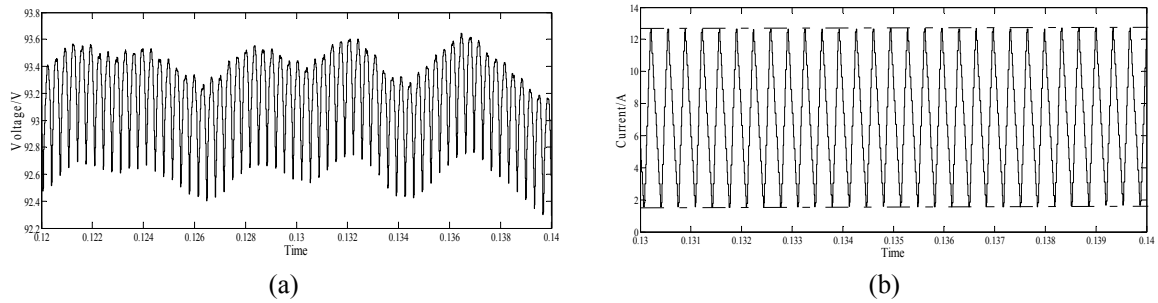


Figure 8. Simulation results for Z-source network for (a) capacitor voltage, and (b) inductor current

7.2. Experimental Results

Real-time laboratory prototype is based on eZdsp™ TMS320F2812DSP. Parameters of the Z-source network, the load and the five phase H-bridge inverter used in the simulation were kept the same as in Table 2. The sampling time used in the experimental setup is similar to that applied in the simulation environment, which is 13 μ sec. The sampling time was chosen as it must be at least twice the highest analog frequency components (1500Hz switching frequency and 50Hz fundamental frequency).

The output voltage is measured for the four phases in the steady state condition and is as shown in Figure 9. The fifth phase is not shown due to the limited number of channels available on the oscilloscope. Figure 10 shows the output voltage and current for Phase A under steady state condition. These results are nearly the same as the ones presented in the simulation. In order to confirm the shoot-through period, which occurred in each leg of the fivephase H-bridge inverter, the PWM signals during the steady state are experimentally measured in real-time, where the PWM signals for S1, S2, S3 and S4 are shown in Figure 11. The PWM signals for S5, S6, S7 and S8 are shown in Figure 12 and the PWM signals for S9 and S10 are shown in Figure 13. The shoot-through condition (indicated in black dotted-circle) can be clearly observed in each leg, where the PWM gate signals of each leg are in the “ON” high state simultaneously, which means that the two switches of the same leg are in the conduction state. Consequently, the output of the fivephase H-bridge inverter is short-circuited and equal to zero.

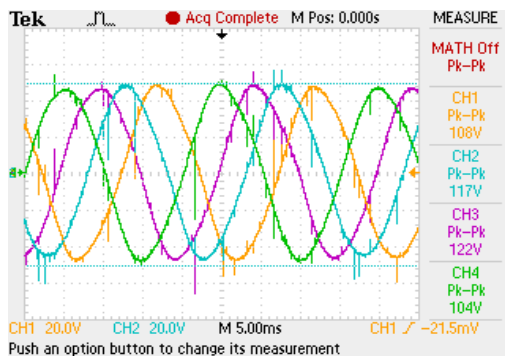


Fig.9 Output voltage for four-phase under $M_i = 0.62$, with 25 ohm resistiveload

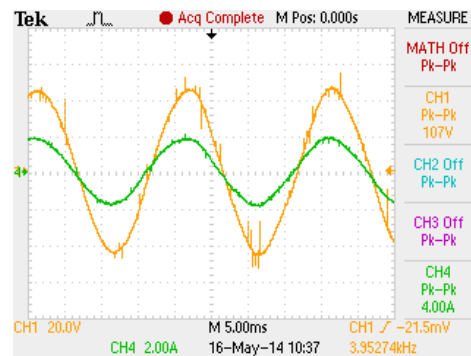


Figure 10. Output voltage (CH1) and output current (CH4) for Phase A under $M_i = 0.62$ with 25 ohm load

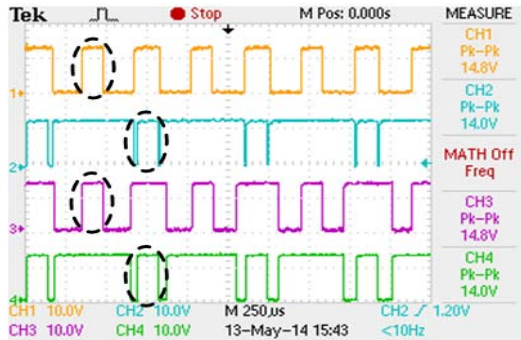


Figure 11. PWM signals for S1 (CH1), S2 (CH2), S3 (CH3) and S4 (CH4)

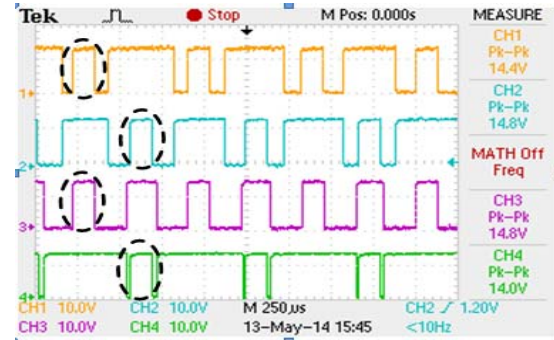


Figure 12. PWM signals for S5 (CH1), S6 (CH2), S7 (CH3) and S8 (CH4)

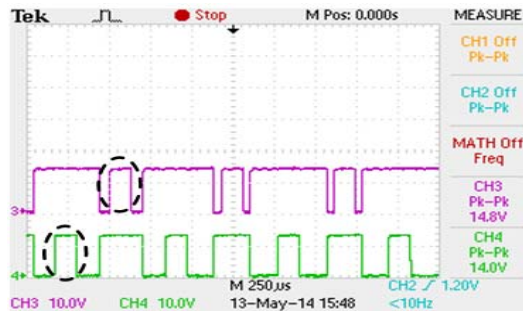


Figure 13. PWM signals for S9 (CH3) and S10 (CH4)

In order to measure the THD, the inverter output current waveform during one fundamental period is recorded using a digital storage oscilloscope TPS2024B. Figure 14 shows the THD for output current of phase A for $M_i = 0.62$ with 25 ohm resistive load. Based on the EN61000-3-2 standard under class D specification, the maximum permissible current of 3rd harmonic is 2.3 A [25]. The data in the oscilloscope are subsequently analyzed using a personal computer to determine the current for the 3rd order harmonic, which is found to be 50mA. Hence, this proved that the result for this research complies with EN61000-3-2 standard.

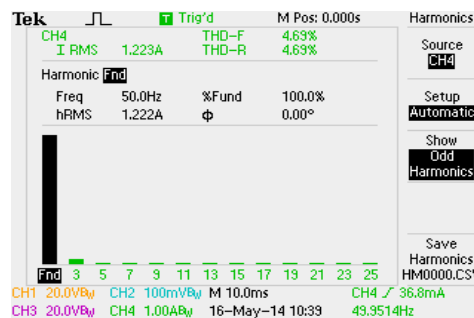


Figure 14. THD output current of phase A under $M_i = 0.62$, with 25 ohm resistive load

Figure 15 shows the $V_{DCLINK} = 162V$ under $M_i = 0.62$ with 25 ohm resistive load compared to 150V achieved in the simulation, as shown in Figure 7. There is a good agreement between the simulated and experimental results as the error between the two is 7%.

The measured capacitor voltage and inductor current under $M_i = 0.62$ with 25 ohm resistive load is shown in Figure 16. Compared to the results obtained from simulation, the error in the capacitor voltage and the inductor current is 8%. As shown in Figure 8(b), the inductor current ripple obtained from the experiment

is 9.2A, which is nearly similar to that obtained from the simulation. This is one feature of SBPWM that produces high DC link voltage.

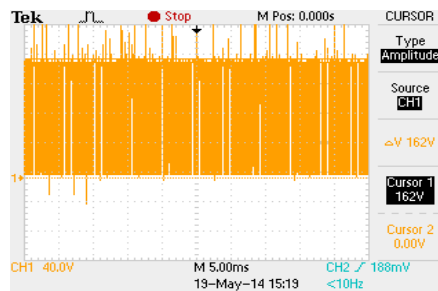


Figure 15. V_{Dlink} under $M_i = 0.62$ with 25 ohm resistiveload

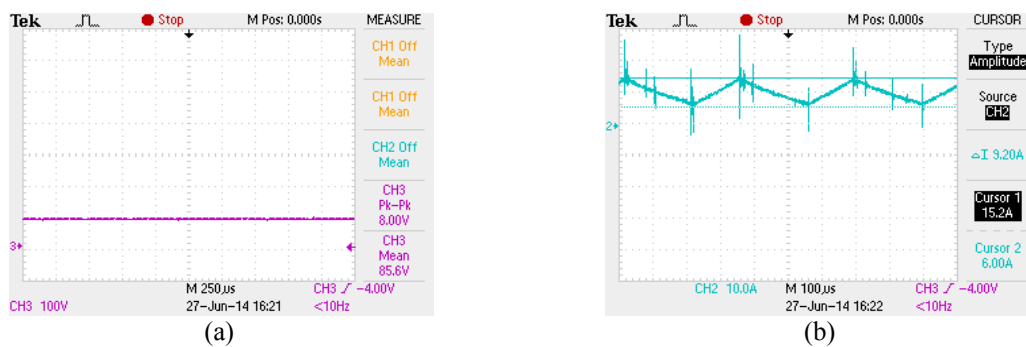


Figure 16. Experimental results for Z-source network: (a) inductor current (CH2), and (b) capacitor voltage (CH3) for Phase A under $M_i = 0.62$ with 25 ohm load

8. CONCLUSION AND FUTURE WORK

In this paper, the performance of SBPWM was investigated and analysed, after which the experimental results were compared with that obtained from simulation. The boosting and bucking mode of ZSI five phase was found to operate as predicted when the modulation index M_i is limited to the range of 0.6 to 1.0. Also, THD of the output current complied with the requirements of EN61000-3-2 standard. It is highly recommended that this work be further studied by investigating the reliability of ZSI five phase under close-loop control.

ACKNOWLEDGEMENTS.

This work was financed by Exploratory Research Grant Scheme (ERGS) under Ministry of Higher Education Malaysia (MOHE), vote number RDU130607. The author thanks University Malaya's Power Energy Dedicated Advanced Centre (UMPEDAC) for placement throughout the research tenure. The authors thank all those involved.

REFERENCES

- [1] E Levi, R Bojoi, F Profumo, HA Toliyat, S Williamson. Multiphase induction motor drives - a technology status review, *Electr. Power Appl. IET*, 2007; 1(4): 489–516.
- [2] PC Loh, DM Vilathgamuwa, Y Sen Lai, GT Chua. Pulse-Width Modulation of Z -Source Inverters, *IEEE Trans. Power Electron*, 2005; 20(6): 1346–1355.
- [3] FZ Peng. Z-Source Inverter, *IEEE Trans. Ind. Appl.*, 2003; 39(2): 504–510.
- [4] VR Rajan, CSA Sekhar, RH Kumar, M Sasikumar, Comparative Evaluation of Generalized Multicell Impedance Source Inverter for Drives, *Int. J. Power Electron. Drive Syst.*, 2014; 4(1): 61–68.
- [5] A Kouzou, H Abu-rub. Multiphase Z-source inverter using maximum constant boost control, *Archives of Control Sciences*, 2013; 23(1): 107–126.
- [6] F Gao, PC Loh, F Blaabjerg, R Teodorescu. *Modulation Schemes of Multi-phase Three-Level Z-Source Inverters*, 2007 IEEE Power Electron. Spec. Conf., 2007; 1905–1911.

- [7] AR Barati, M Moslehi, DA Khaburi. *Z-Source Five Leg Inverter*, 4th Power Electronics, Drive Systems & Technologies Conference (PEDSTC2013), 2013; 2(1): 205–211.
- [8] PA. Dahono, S Member, EG Supriatna. Output Current-Ripple Analysis of Five-Phase PWM Inverters, *IEEE Trans. Ind. Appl.*, 2009; 45(6): 2022–2029.
- [9] MJ Drazen Dujic, EL Slobodan, N Vukosavic. A General PWM Method for a $(2n + 1)$ -Leg Inverter Supplying n Three-Phase Machines, *IEEE Trans. Ind. Electroncis*, 2009; 56(10): 4107–4118.
- [10] S Thangaprakash, A Krishnan. Comparative evaluation of modified pulse width modulation schemes of Z-source inverter for various applications and demands, *Int. J. Eng. Sci. Technol.*, 2010; 2(1): 2005–2008.
- [11] Z Miao, Y Kun, L Fang Lin. Topology analysis of a switched-inductor Z-source inverter, *Industrial Electronics and Applications (ICIEA)*, 2010; 364–369.
- [12] Y Tang, S Xie, C Zhang, Z Xu. Improved Z-Source Inverter With Reduced Z-Source Capacitor Voltage Stress and Soft-Start Capability, *IEEE Trans. Power Electron.*, 2009; 24(2): 2005–2008.
- [13] X Ding, C Zhang, Z Qian. *X-source inverter: A generic Z-source inverter structure*, 2013 IEEE Energy Conversion Congress and Exposition, 2013; 5341–5348.
- [14] LJ Sumedha Rajakaruna. Steady-State Analysis and Designing Impedance Network of Z-Source Inverters, *IEEE Trans. Ind. Electroncis*, 2010; 57(7): 2483–2491.
- [15] O Ellabban, S Member, J Van Mierlo, and P. Lataire. *Voltage Mode and Current Mode Control for a 30 kW High-Performance Z-Source Inverter*, Electrical Power & Energy Conference, 2009; Vm.
- [16] V Tran-Quang, C Tae-Won, HG Kim, EC Nho. Minimization of Voltage Stress Across Switching Devices in The ZSI by Capacitor Voltage Control, *J. Power Electron*, 2009; 9(3): 335–342.
- [17] B Nayak, SS Dash, S Kumar. Proposed Method for Shoot-Through in Three Phase ZSI and Comparison of Different Control Techniques, *Int. J. Power Electron. Drive Syst.*, 2014; 5(1): 32–40,.
- [18] M Shen, W Jin, A Joseph, FZ Peng, LM Tolbert, DJ Adams. *Maximum constant boost control of the Z-source inverter*, Industry Applications Conference, 39th IAS Annual Meeting. Conference Record of the 2004 IEEE, 2004; 1: 147.
- [19] S Thangaprakash, A Krishnan. Implementation and Critical Investigation on Modulation Schemes of Three Phase Impedance Source Inverter, *Iran. J. Electr. Electron. Eng.*, 2010; 6(2), 84–92.
- [20] S Miaosen, P Fang Zheng. Operation Modes and Characteristics of the Z-Source Inverter With Small Inductance or Low Power Factor, *Ind. Electron. IEEE Trans.*, 2008 55(1) 89–96.
- [21] DSPD. Systems, *eZdsp TM F28335 Technical*, 2007.
- [22] M Mansor, NA Rahim, Three-Phase PWM-Switched Autotransformer Voltage-Sag Compensator Based on Phase Angle Analysis, *J. Power Electron.*, 2011; 11(6): 897–903.
- [23] M Abdullah, A Abu Talib, N Mohd Suradi, A Mokhtar, N Jamaluddin, M Zainuddin. *K-Chart: Research Planning and Monitoring Tool For Engineering and Technology Applications*, FEIIC Seminar on Engineering and Technology, 2006.
- [24] H Daniyal. Investigation of Digital Current Control Based on Zero Average Current Error Concept, The University of Western Australia, 2010.
- [25] EPSMA. (EPSMA). *Harmonic Current Emissions Guidelines to the standard EN 61000-3-2 Revision Date : 2010-11-08*, 2010.

BIOGRAPHIES OF AUTHORS



Mohd. Shafie Bakar was born in Johor, Malaysia, in 1972. He received his Bachelor of Engineering in Electronics from Oxford Brookes University in 1996 and Master in Electrical Engineering from Universiti Teknologi Malaysia in 2003. Currently he is doing PhD with Faculty of Electrical & Electronics Engineering, Universiti Malaysia Pahang. He is currently a lecturer at Sustainable Energy & Power Electronics (SuPER), Faculty of Electrical & Electronics Engineering, Universiti Malaysia Pahang. His research interests include power converters, battery management systems and renewable energy systems. Mr Mohd Shafie is a member of IET, IEM and Board of Engineer, Malaysia



Nasrudin Abd. Rahim (M'89-SM'08) was born in Johor, Malaysia, in 1960. He received his B.Sc. (Hons.) and his M.Sc. degrees from the University of Strathclyde, Glasgow, U.K., and his Ph.D. degree in 1995 from Heriot-Watt University, Edinburgh, U.K. He is currently a Professor with the Department of Electrical Engineering, University of Malaya, Kuala Lumpur, Malaysia and the Director of the UM Power Energy Dedicated Advanced Centre. Dr. Rahim is a Fellow of the Institution of Engineering and Technology, U.K. and a Chartered Engineer. He is also Chairman of the Working Group WG-8, covering reluctance motors, of the IEEE Motor Subcommittee under IEEE Power Engineering Society/Electric Machinery Committee. His research interests include power electronics, real-time control systems, and electrical drives



Hamdan Daniyal (S'07–M'11) was born in N.Sembilan, Malaysia, in 1980. He received the B.Eng. degree in electrical and electronics from Universiti Teknologi Malaysia in 2002, the M.Eng. degree in mechatronics from Kolej Universiti Teknologi Tun Hussein Onn, Malaysia, in 2004, and the Ph.D. degree in digital current control for power electronics converter from The University of Western Australia, Perth, Australia, in 2011. In 2002, he was an Electrical and Electronics Engineer with Smart Ind., a switched-mode power-supply manufacturing company. Later in 2003, he joined Universiti Malaysia Pahang (formerly known as KUKTEM) as a Lecturer. After completing his doctoral work, he became one of the key people with the Sustainable Energy & Power Electronics Research (SuPER) Group, Universiti Malaysia Pahang. His research interest include switching strategy, nonlinear control and digital control in power electronics applications such as renewable energy, electric vehicle, battery management, power quality, and active power filters. Dr. Daniyal is a member of the IEEE Power Electronics Society and the IEEE Industrial Electronics Society.



Kamarul Hawari Ghazali was born in Selangor, Malaysia in 1973. He received the B.E.E. and M.E.E. from Universiti Teknologi Malaysia and Ph.D. from Universiti Kebangsaan Malaysia in 2009. He is currently an Associate Professor at Faculty of Electrical & Electronics Engineering in Universiti Malaysia Pahang. He serves as a lecturer of numerous short courses to industry as his expertise in machine vision and thermal imaging analysis. His current research interests include digital image processing in the application of automation, agriculture, industrial electronics and military. Assoc. Prof Dr. Kamarul Hawari is a member of Board of Engineers Malaysia